IL NUOVO CIMENTO **38 C** (2015) 67
DOI 10.1393/ncc/i2015-15067-4

Communications: SIF Congress 2014

Cold-atom interferometry: A tool for metrology and fundamental physics

G. Rosi

Dipartimento di Fisica e Astronomia & LENS, Università di Firenze,
INFN, Sezione di Firenze - via Sansone 1, I-50019 Sesto Fiorentino (FI), Italy

received 20 February 2015

Summary. — In this paper, after a short theoretical introduction, we are going to discuss the application of matter-wave interferometry to the precise measurement of two important physical constants: the Newtonian gravitational constant G and the fine-structure constant α. This capability of determining the strength of so different fundamental interactions (gravity and electromagnetism) makes such technique one of the most versatile investigation methods available.

PACS 37.25.+k – Atom interferometry techniques.
PACS 06.20.-f – Metrology.

1. – Introduction

Nowadays interference with matter waves [1] is a rich branch of atomic physics and quantum optics. Starting from the first matter-wave interferometers based on slow neutrons diffracted by crystal planes [2], such technique has evolved over the years towards the use of cold atomic samples manipulated by light fields. The first proof-of-principle experiment of such scheme was realized in 1991 by the group of Steven Chu in Stanford [3] measuring the local gravity acceleration; eight years later it was improved in accuracy and sensitivity by the same group [4], reaching astonishing precision levels, comparable to if not better than, state of the art classical instruments. From this seminal work several kinds of gravity and inertial-force–based measurements have been performed, in particular: Earth gravity gradient [5,6], local gravity curvature [7], rotations [8] and Newtonian gravitational constant G [9-11]. In parallel, an apparatus devoted to non-gravitational experiments has been conceived and realized especially concerning the fine-structure constant α [12, 13]. The basic ingredient of all these instruments lies in the realization of the so-called Mach-Zehnder interferometer. Such kind of scheme is achieved using a $\pi/2$-π-$\pi/2$ sequence of three Raman pulses in counterpropagating configuration that couples the two hyperfine ground states (labeled as a and b, see fig. 1) of an alkali atom (usually Cs or Rb) and trasfers at the same time a momentum $\hbar k_{\text{eff}}$, where k_{eff} is the

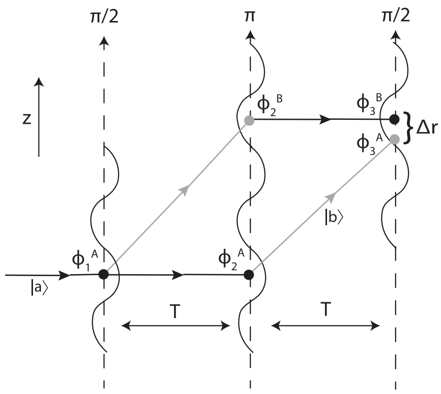

Fig. 1. – Basic Mach-Zehnder–type atom interferometer without gravity. Initially the atomic wave packet is put into a superposition of hyperfine ground states using stimulated Raman transitions ($\pi/2$ pulse). During this process a momentum $\hbar k_{\text{eff}}$ is also transferred to the atom, thus realizing a beam splitter for matter waves; at a time $t = T$ a second pulse (π pulse) redirects the wave packets performing a state inversion, playing the role of a mirror; finally, at $t = 2T$, the final $\pi/2$ pulse recombines the wave packts producing the interference. Phase terms due to light interaction are indicated on each path and fictitious path separation has been introduced for illustrative purposes. Internal states are indicated with different shades of gray.

Raman lasers wave vectors. In this picture the $\pi/2$ and π pulses realize respectively the beam-splitters and mirrors of the interferometer (see fig. 1). At the interferometer output, the probability of detecting the atoms in the given internal state $|a\rangle$ is given by $P_a = (1 + \cos(\phi))/2$, where ϕ represents the phase difference accumulated by the wave packets along the two interferometer arms. Such quantity can be theoretically evaluated and different approaches have been developed for this purpose. Here we are going to consider the one that makes use of the path integral formalism [14]. According to this last description ϕ is given by the sum of three contributions:

$$\phi = \phi_F + \phi_I + \phi_S \tag{1}$$

The first one is obtained calculating the classical Lagrangian action $S_F = \int L\mathrm{d}t$ along each interferometer path (labeled here with A and B) and evaluating

$$\phi_F = \frac{1}{\hbar}(S_F^B - S_F^A). \tag{2}$$

The second term takes into account the additional phase shifts due to the interactions with the light fields:

$$\phi_I = \sum_{PathB} \varphi_j - \sum_{PathA} \varphi_i, \tag{3}$$

where $\varphi_{i(j)}$ is the local Raman phase at which an atom along a given path is subjected at the interrogation instant. Finally the third term is associated to the fact that the two wave packets going through two arms of the interferometer may not overlap perfectly:

$$\phi_S = \frac{\mathbf{p} \cdot \mathbf{\Delta r}}{\hbar}, \tag{4}$$

here $\mathbf{p}$ is the average atomic momentum at the interferometer output and $\mathbf{\Delta r}$ is the spatial separation of the two wave packets. Applying these calculations to a free particle in constant gravity field we have

$$\phi = (k_{\text{eff}} g - \beta) T^2, \tag{5}$$

where g, T and β are respectively the local gravity acceleration, the free evolution time and the Raman lasers frequency chirp rate to compensate the Doppler frequency shift. The overall phase shift comes only from the ϕ_I contribution, while ϕ_F and ϕ_S are equal to zero. The g value can be inferred from the β value that leads to $\phi = 0$ for every T value.

In more involved cases where the Lagrangian L contains high-order terms in position and/or in momentum, the above procedure can be mathematically very complex to pursue. If we can express L as the sum of an unperturbed term L_0 and a L_1 term containing all the high-order terms and the condition $|L_1/L_0| \ll 1$ holds along the particle trajectory, a perturbative approach can be employed [14] yielding to an extra phase shift ϕ_{pert} given by

$$\phi_{pert} = \frac{1}{\hbar} \int_{\Gamma_0} L_1 \mathrm{d}t, \tag{6}$$

where Γ_0 is the unperturbed particle path. Now, having in mind this theoretical background, we are going to present two successful applications of atom interferometry, the measurement of the gravitational constant G and the fine structure constant α, briefly discussing the different schemes implemented over the years. Technical details of the experiments will be omitted.

2. – Measurement of the Newtonian gravitational constant

Nowadays most of the physical constants are known within a few parts per billion, in the worst cases some parts per million. One of the few exceptions is the gravitational constant G, introduced for the first time by Newton in 1665 to describe the attractive force between all bodies with mass. Despite

$$\mathbf{F} = -G \frac{m_1 m_2}{r^3} \mathbf{r} \tag{7}$$

being one of the best known among all physical laws, the last CODATA-recommended value of G has still a relative uncertainty of 120 ppm. Besides the purely metrological interest, there are several reasons why a more precise determination of G is important: in astronomy, the factor GM of astronomical objects can be determined extremely well and thus a better knowledge of G leads to a better knowledge of M, which in turn leads to a better physical understanding of celestial bodies; in geophysics, uncertainties of density and elastic parameters of the Earth are directly related to the uncertainties on

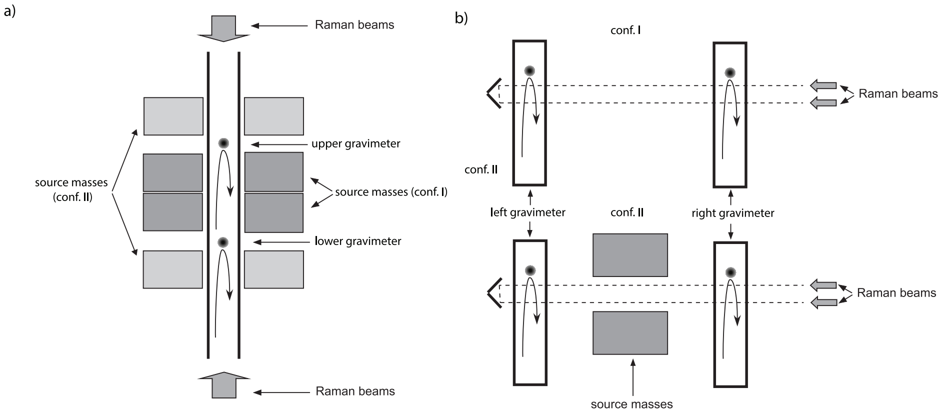

Fig. 2. – (a) Atomic gravity gradiometer in vertical configuration. Two vertical displaced atomic samples are interrogated by vertical Raman beams in counterpropagating configuration in order to realize two simultaneous interferometers. External source masses are positioned in two different configurations (I and II) and the induced phase shift is measured as a function of mass positions. (b) Atomic gravity gradiometer in horizontal configuration. Again, two horizontal displaced atomic samples are simultaneously interrogated by horizontal Raman beams in counterpropagating configuration. The Raman light propagates in free space through both sensors and reflects from a corner cube defining in this way two transversal regions for the $\pi/2$ and π pulses. The horizontal gradient is produced adding source masses (configuration II) between the sensors.

G; in theoretical physics, spatial variations of G are predicted by some theories; moreover, string theory assumes additional dimensions rolled up at small distances, causing a breakdown of the inverse square law of gravity. The reasons for the difficulties in the determination of G can be found in the completely different nature of the gravitational force: gravity cannot be shielded or compensated for and its weakness allows other forces to contribute with big systematic effects in laboratory experiments. Secondly, the majority of the experiments performed so far are based on macroscopic suspended masses: parasitic couplings in suspending fibers are not well understood and could be responsible for the observed discrepancies. Instead, using microscopic masses as neutral atoms to probe the gravitational field generated by a well characterized source mass can solve this kind of problems. For all these reasons, atom interferometry represents an alternative and powerful method.

In fig. 2 two kinds of experimental implementations devoted to this purpose are depicted. Both are gravity gradiometers, one of them is vertical, the other horizontal [15]. The measurement principle is basically the same, so in the following we will describe in detail the first solution and afterwards we will put in evidence some special features of the second scheme. A gravity gradiometer can be obtained by two vertically displaced Mach-Zehnder interferometers, realized by Raman interrogation of two free falling atomic samples. Each gravity sensor measures the local acceleration with respect to the common reference frame identified by the wavefronts of the Raman lasers. Therefore, even in presence of a strong phase noise that completely washes out the atom interference fringes, the signals simultaneously detected on the upper and lower accelerometers remain coupled and preserve a fixed-phase relation. As a consequence, when the trace of the upper accelerometer is plotted as a function of the lower one, experimental points distribute along a Lissajous ellipse. The differential phase shift $\Phi = \phi_{up} - \phi_{dw}$, which is proportional to the gravity gradient, is then obtained from the eccentricity and the rotation angle of the ellipse best fitting the experimental data [16]. In order to modulate the actual value of the gravity gradient, a set of source masses are vertically displaced in two different configurations, in order to reduce it (configuration I) and enhance it (configuration II). The induced phase shift is thus measured as a function of masses positions, realizing in this way a double differential scheme, suitable to isolate the effect of source masses from others biases of acceleration difference between the two clouds (Earth's gravity gradient, Coriolis forces, etc.). Knowing all the geometric parameters of the atomic sample and source masses distribution, the value of G can be determined, being directly proportional to the differential angle

$$\Delta\Phi = \Phi_{II} - \Phi_{I}. \tag{8}$$

This value can indeed be numerically evaluated using eq. (6), leaving in this way G as the unique free parameter.

After some proof-of-principle measurements [9,10], recently the described solution has lead to a precision measurement with 150 ppm of relative uncertainty [11], which is for the first time comparable with that of the current CODATA value.

An alternative approach, described for the first time in [15], is the use of a gravity gradiometer in horizontal configuration. The measurement protocol is almost the same: again, two simultaneous, horizontally displaced Mach-Zehnder interferometers are realized by Raman pulse interrogation. This time the k_{eff} vector is perpendicular with respect to the gravity and consequently to the atomic parabolic motion. For this reason it is necessary to create two vertically separated interrogation zones, one for the $\pi/2$ pulses (clouds ascension and fall) and the other for the π pulse at the trajectories apogee. A corner cube reflector guarantees the parallelism of the two beam levels. The quantity $\Delta\Phi$ is retrieved measuring the gradiometer phase with (configuration II) and without (configuration I) the presence of source masses between the two accelerometers. Preliminary measurements demonstrated a statistical relative uncertainty on G of 3×10^{-4}, forecasting a final sensitivity down to 1×10^{-6} with appropriate technical updates. Finally it is important to underline that in such scheme the gradiometer phase shift is totally due to the source masses only, while in a vertical gradiometer a consistent portion of the phase comes from the gravity gradient. This characteristic makes the horizontal setup superior in performing test of the Newton's Inverse Square Law by directly measuring the spatial dependence of the gravitational field. New experiments devoted to improve the state-of-art constraints on Yukawa-type force in the 10 cm range appear to be feasible.

3. – Measurement of the ratio h/m and the determination of the fine-structure constant

The fine-structure constant, commonly denoted α, is a fundamental physical constant, namely the coupling constant characterizing the strength of the electromagnetic interaction between elementary charged particles. It plays a central role in Physics, mainly for three reasons: it represents the most accurate test of theories such as quantum electrodynamics (QED) [17], it is a valid benchmark for testing the stability of fundamental constants [18] and its value can be a key ingredient in the redefinition of the kilogram in the international system of units (SI) [19]. In 1994 the group of S. Chu has developed a

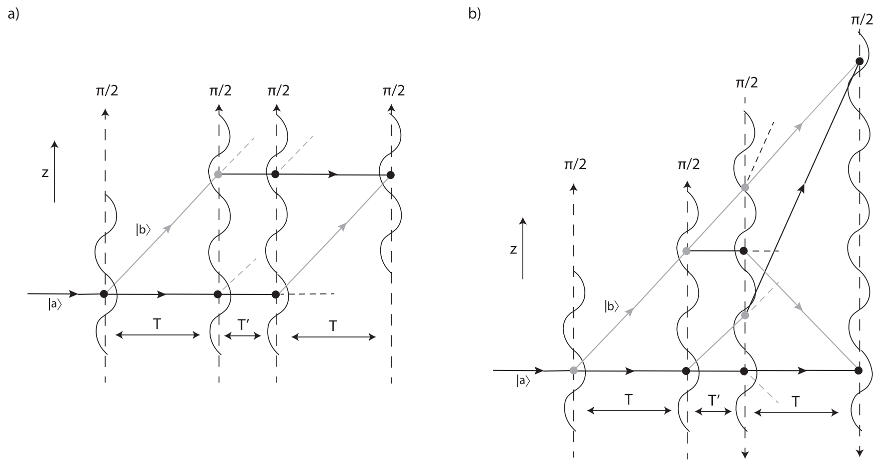

Fig. 3. – (a) Symmetric Ramsey-Bordé interferometer. After the first $\pi/2$ pulse pair, wave packets along interferometer arms are in the same momentum state, enabling the possibility to accelerate them using, for istance, Bloch oscillations. (b) Asymmetric Ramsey-Bordé interferometer. Internal states are indicated with different shades of gray. Paths that do not interfere at the final light pulse are prematurely truncated, in order to highlight the two pairs which do interfere.

new measurement method, based on the determination of the ratio h/m_X, between the Planck constant h and the atomic mass m_X. This ratio is related to α by

$$\alpha^2 = \frac{2R_\infty}{c}\frac{A_r(X)}{A_r(e)}\frac{h}{m_X}. \tag{9}$$

The Rydberg constant R_∞ is known with an accuracy of 5×10^{-12} [20] while the quantities $A_r(e)$ (the relative atomic mass of the electron) and $A_r(e)$ (the relative atomic mass of a X element) are known with uncertainties below 10^{-10} (if X = Rb or Cs [21,22]), leaving $\frac{h}{m_X}$ the factor with the largest error. The ratio h/m is deduced from the measurement of the recoil velocity of an alkali atom, usually ^{133}Cs or ^{87}Rb, which absorbs or emits a photon, and the frequency of the photon involved. Atom interferometry can be implemented in order to perform such kind of experiment. Here we will present two interferometer geometries, both of them based on a $\pi/2$-$\pi/2$-$\pi/2$-$\pi/2$ pulses sequence.

The first one, called Symmetric Ramsey-Bordé interferometer, can be thought of as a generalization of the Mach-Zehnder scheme where the central π pulse is substituted by two $\pi/2$ pulses temporally spaced by a time T' (see fig. 3, left part). The resulting phase shift, considering a free particle in a constant gravity field, is thus

$$\phi = (k_{eff}g - \beta)(T + T')T + (k_{\text{eff}}\Delta v + \Delta\omega)T, \tag{10}$$

where the term Δv allows for any non-gravitational velocity variation of the two interferometer arms between the second and the third pulses, $\Delta\omega$ is the frequency jump needed to keep the Raman lasers at resonance with the atoms. Also in this case only ϕ_I contributes to the phase.

Bloch oscillations in a one-dimensional lattice [23] is the privileged technique to produce a well-controlled velocity change

$$\Delta v = 2N v_r \tag{11}$$

with v_r the velocity recoil of the atom in the lattice and N the oscillations number. Again, imposing the condition $\phi = 0$ for each (T, T') couple, we can determine $\Delta\omega = -\Delta v k_{\rm eff}$ and finally

$$\frac{h}{m} = \frac{-\Delta\omega}{2N k_{\rm eff} k_{lattice}}. \tag{12}$$

Such combination of Raman interferometry and Bloch oscillations, together with several precautions in order to reduce systematic effects, has lead to a determination of the fine constant with a relative accuracy of 0.66 ppb [24].

The second geometry, the asymmetric Ramsey-Bordé interferometer, proposed in [25] and experimental demonstrated for the fist time in [12], presents some special features that need to be highlighted. In this case the second pair of Raman $\pi/2$ pulses are $k_{\rm eff}$ reversed, in order to close simultaneously two interferometer paths, as described in fig. 3, right part. Thus, the expression of the phase shift for the upper (ϕ^+) and the lower (ϕ^-) interferometer becomes

$$\phi^{\pm} = (k_{\rm eff}\, g - \beta)(T + T')T + (k_{\rm eff}\Delta v^{\pm} + \Delta\omega^{\pm})T \pm \phi_F, \tag{13}$$

where this time $\phi_F = 2E_{kin}T/h = \hbar k_{\rm eff}^2 T/m \simeq 8\omega_r T$ differs from zero, because of the difference in kinetic energy E_{kin} between the interferometer arms. Moreover, considering the quantity $\Phi = \phi^+ - \phi^-$, it is possible to get rid of the gravitational contribution, bringing down systematic effects. Moreover, the simultaneous interrogation of two interferometers can suppress the phase noise, as discussed in the previous section. Similarly to the symmetric case, to gain sensitivity on the recoil frequency ω_r, it should be convenient to enhance the $\Delta v^{\pm}$ term by accelerating upward/downward the upper/lower interferometer. Unfortunately in this condition the Raman beams cannot address both the them at the same time, losing one of the main advantages of the asymmetric configuration. A possible trivial solutions to this issue can be the introduction of a second Raman beams pair. Also alternating in time the realization of the two interferometers can be effective, even if the simultaneity of the interrogation is lost.

Recently an updated version of such scheme, based on multi-photon Bragg transitions to maximize the wave-packets separation [26] and Bloch oscillations to obtain a large Δv term, has been developed by the group of H. Müller at Berkeley University. Preliminary measurements have already demonstrated an accuracy level of 2.0 ppb [27] and a sensitivity of 0.33 ppb after 6 hours of integration [28] paving the way towards a new determination of the fine-structure constant.

4. – Conclusion and outlooks

In this paper we have briefly described schemes and recent results about precision measurements of the Newtonian gravitational constant G and the fine-structure constant α by cold-atom interferometry, pointing out the unique ability of such technique to probe gravity as well as key features of the electromagnetic interaction. Further improvements in the accuracy level of both the constants are envisaged [15, 28], yielding potentially to significant advantages in metrology and fundamental physics. Finally it is worth mentioning that many other results are expected from ongoing atom interferometry experiments, ranging from new verifications of the Weak Equivalence Principle [29,30] to short-distance tests of Newton's $1/r^2$ Law [15]. Moreover future ambitious setup devoted to the gravitational waves detection has been also proposed [31].

* * *

The author acknowledges G. M. Tino for a critical reading of the manuscript.

REFERENCES

[1] Tino G. M. and Kasevich M. (Editors), *Proc. Int. School Phys. "Enrico Fermi", Course CLXXXVIII* (Societa' Italiana di Fisica and IOS Press) 2014.
[2] Fermi E. and Marshall L., *Phys. Rev.*, **71** (1947) 666.
[3] Kasevich M. and Chu S., *Phys. Rev. Lett.*, **67** (1991) 181.
[4] Peters A., Chung K. Y. and Chu S., *Nature*, **400** (1999) 849.
[5] McGuirk J. M., Foster G. T., Fixler J. B., Snadden M. J. and Kasevich M. A., *Phys. Rev. A*, **65** (2002) 033608.
[6] Sorrentino F., Lien Y.-H., Rosi G., Cacciapuoti L., Prevedelli M. and Tino G. M., *New J. Phys.*, **12** (2010) 095009.
[7] Rosi G., Cacciapuoti L., Sorrentino F., Menchetti M., Prevedelli M. and Tino G. M., *Phys. Rev. Lett.*, **114** (2015) 013001.
[8] Gauguet A., Canuel B., Lvque T., Chaibi W. and Landragin A., *Phys. Rev. A*, **80** (2009) 063604.
[9] Fixler J. B., Foster G. T., McGuirk J. M. and Kasevich M. A., *Science*, **315** (2007) 74.
[10] Lamporesi G., Bertoldi A., Cacciapuoti L., Prevedelli M. and Tino G. M., *Phys. Rev. Lett.*, **100** (2008) 050801.
[11] Rosi G., Sorrentino F., Cacciapuoti L., Prevedelli M. and Tino G. M., *Nature*, **510** (2014) 518.
[12] Weiss D. S., Young B. C. and Chu S., *Appl. Phys. B*, **59** (1994) 217.
[13] Wicht A., Hensley J., Sarajlic E. and Chu S., *Phys. Scr.*, **T102** (2002) 82.
[14] Storey P. and Cohen-Tannoudji C., *J. Phys. II France*, **4** (1994) 1999.
[15] Biedermann G. W., Wu X., Deslauriers L., Roy S., Mahadeswaraswamy C. and Kasevich M., arXiv:1412.3210 (2014).
[16] Foster G. T., Fixler J. B., McGuirk J. M. and Kasevich M., *Opt. Lett.*, **27** (2002) 951.
[17] Aoyama T., Hayakawa M., Kinoshita T. and Nio M., *Phys. Rev. Lett.*, **109** (2012) 111807.
[18] Uzan J. P., *Living Rev. Relativ.*, **14** (2011) 2.
[19] Mills I. M., Mohr P. J., Quinn T. J., Taylor B. N. and Williams E. R., *Philos. Trans. R. Soc. A*, **369** (2011) 3907.
[20] Mohr P. J., Taylor B. N. and Newell D. B., *Rev. Mod. Phys.*, **80** (2008) 633.
[21] Bradley M. P., Porto J. V., Rainville S., Thompson J. K. and Pritchard D. E., *Phys. Rev. Lett.*, **83** (1999) 4510.
[22] Mount B. J., Redsha M. and Myers E. G., *Phys. Rev. A*, **82** (2010) 042513.
[23] Ferrari G., Poli N., Sorrentino F. and Tino G. M., *Phys. Rev. Lett.*, **97** (2006) 060402.
[24] Bouchendira R., Cladé P., Guellati-Khelifa S., Nez F. and Biraben F., *Phys. Rev. Lett.*, **106** (2011) 080801.
[25] Bordé C. J., *Phys. Lett. A*, **140** (1989) 10.

[26] Muller H., Chiow S.-W., Long Quan, Herrmann Sven and Chu S., *Phys. Rev. Lett.*, **100** (2008) 180405.
[27] Lan S. Y., Kuan P. C., Estey B., English D., Brown J. M., Hohensee M. A. and Muller H., *Science*, **339** (2013) 554.
[28] Estey B., Yu C., Muller H., Kuan P.-C. and Lan S.-Y., arXiv:1410.8486 (2014).
[29] Schlippert D., Hartwig J., Albers H., Richardson L. L., Schubert C., Roura A., Schleich W. P., Ertmer W. and Rasel E. M., *Phys. Rev. Lett.*, **110** (2013) 171102.
[30] Tarallo M. G., Mazzoni T., Poli N., Sutyrin D. V., Zhang X. and Tino G. M., *Phys. Rev. Lett.*, **113** (2014) 023005.
[31] Graham P. W., Hogan J. M., Kasevich M. and Rajendran S., *Phys. Rev. Lett.*, **110** (2013) 171102.